Metabolic Engineering Communications 7 (2018) e00073

Contents lists available at ScienceDirect

Metabolic Engineering Communications

journal homepage: www.elsevier.com/locate/mec

Engineering redox-balanced ethanol production in the cellulolytic and extremely thermophilic bacterium, *Caldicellulosiruptor bescii*

Amanda M. Williams-Rhaesa[a], Gabriel M. Rubinstein[a], Israel M. Scott[a], Gina L. Lipscomb[a], Farris L. Poole, II[a], Robert M. Kelly[b], Michael W.W. Adams[a,*]

[a] Department of Biochemistry and Molecular Biology, University of Georgia, Athens, GA 30602, USA
[b] Department of Chemical and Biomolecular Engineering, North Carolina State University, Raleigh, NC, USA

ARTICLE INFO

Keywords:
Biofuel
Consolidated bioprocessing
Ferredoxin
Ethanol
Thermophile
C. bescii

ABSTRACT

Caldicellulosiruptor bescii is an extremely thermophilic cellulolytic bacterium with great potential for consolidated bioprocessing of renewable plant biomass. Since it does not natively produce ethanol, metabolic engineering is required to create strains with this capability. Previous efforts involved the heterologous expression of the gene encoding a bifunctional alcohol dehydrogenase, AdhE, which uses NADH as the electron donor to reduce acetyl-CoA to ethanol. Acetyl-CoA produced from sugar oxidation also generates reduced ferredoxin but there is no known pathway for the transfer of electrons from reduced ferredoxin to NAD in *C. bescii*. Herein, we engineered a strain of *C. bescii* using a more stable genetic background than previously reported and heterologously-expressed *adhE* from *Clostridium thermocellum* (which grows optimally (T_{opt}) at 60 °C) with and without co-expression of the membrane-bound Rnf complex from *Thermoanaerobacter* sp. X514 (T_{opt} 60 °C). Rnf is an energy-conserving, reduced ferredoxin NAD oxidoreductase encoded by six genes (*rnfCDGEAB*). It was produced in a catalytically active form in *C. bescii* that utilized the largest DNA construct to be expressed in this organism. The new genetic lineage containing AdhE resulted in increased ethanol production compared to previous reports. Ethanol production was further enhanced by the presence of Rnf, which also resulted in decreased production of pyruvate, acetoin and an uncharacterized compound as unwanted side-products. Using crystalline cellulose as the growth substrate for the Rnf-containing strain, 75 mM (3.5 g/L) ethanol was produced at 60 °C, which is 5-fold higher than that reported previously. This underlines the importance of redox balancing and paves the way for achieving even higher ethanol titers in *C. bescii*.

1. Introduction

The need for sustainable liquid fuel production continues to grow as environmental impacts of fossil fuel use become more apparent (Demain, 2009). In order to overcome these consequences, use of renewable resources must increase. Lignocellulose is an attractive feedstock for biofuel production as it is highly abundant, does not compete with food supplies, and can be generated in sustainable ways (Lynd et al., 2017). However, there are a number of challenges to using lignocellulose for biofuel production, most significantly the recalcitrance of plant biomass to deconstruction and the costs associated with pretreatment and the enzymatic hydrolysis of the plant wall polysaccharides (Brethauer and Studer, 2015). One potential way to minimize these costs is the use of consolidated bioprocessing (CBP) in which enzyme production, polysaccharide hydrolysis and sugar fermentation are all performed by the same microorganism in the same reaction vessel (Lynd et al., 2005; Olson et al., 2012).

The extremely thermophilic bacterium, *Caldicellulosiruptor bescii,* is of great interest for use as a CBP microbe as it has the highest growth temperature of any known cellulolytic bacterium (Yang et al., 2009). Moreover, it is capable of robust growth on a variety of carbon sources, including mono- and polysaccharides of both hexose and pentose sugars, as well as crystalline cellulose and plant biomass without pretreatment even at high solids loadings (Basen et al., 2014; Yang et al., 2009; Zurawski et al., 2017). *C. bescii* ferments these substrates to acetate, lactate, carbon dioxide and hydrogen (Yang et al., 2009). *C. bescii* is also amenable to metabolic engineering as a genetic system is available and has been used to construct strains with multiple gene deletions (Cha et al., 2013) and for heterologous expression of genes both from replicating plasmids (Chung et al., 2013; Scott et al., 2015) and chromosomal integrations (Chung et al., 2014a; Conway et al., 2016; Lipscomb et al., 2016; Williams-Rhaesa et al., 2017). These studies have resulted in an increased understanding of the primary metabolism of *C. bescii* and its mechanisms of plant biomass utilization

* Corresponding author.
E-mail address: adamsm@uga.edu (M.W.W. Adams).

https://doi.org/10.1016/j.mec.2018.e00073
Received 1 November 2017; Received in revised form 16 May 2018; Accepted 27 May 2018

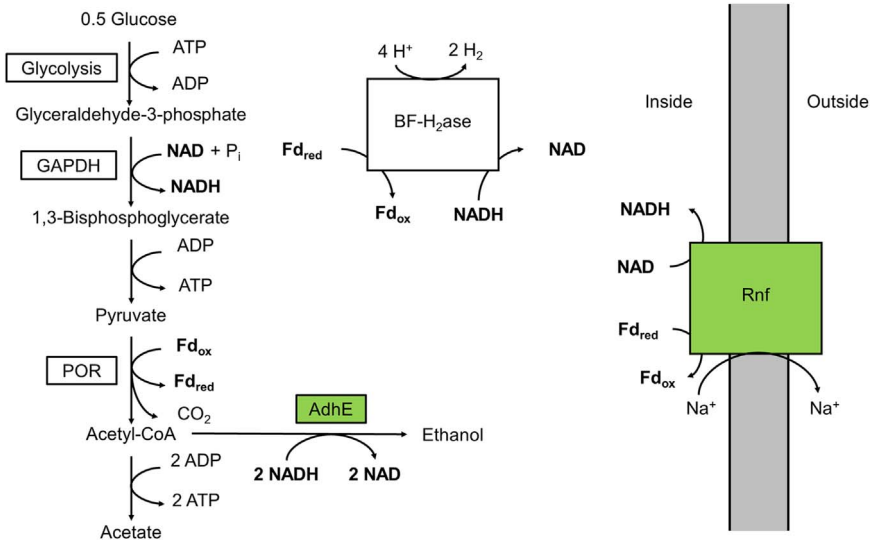

Fig. 1. Pathway for redox balanced ethanol production in *C. bescii*. The AdhE from *C. thermocellum* requires two NADH to generate ethanol from acetyl-CoA, but glycolysis in *C. bescii* generates one NADH and one reduced ferredoxin (Fd_{red}). The heterologous expression of Rnf allows for the transfer of electrons from reduced ferredoxin to NAD to generate the additional NADH needed for redox balanced ethanol production.

(Chung et al., 2014b; Conway et al., 2017). While the original genetic system has been useful, genome instability of the resulting recombinant strains was observed due to an active transposon, IS*Cbe4* (Williams-Rhaesa et al., 2017). A genetically-tractable strain generated through the use of a kanamycin resistance gene was therefore constructed and this has been shown to be much more stable (Lipscomb et al., 2016; Williams-Rhaesa et al., 2017).

In a previous study, the gene (*adhE*) encoding the bifunctional alcohol dehydrogenase from the bacterium *Clostridium thermocellum,* which grows optimally (T_{opt}) at 60 °C (Ng et al., 1977), was heterologously-expressed in *C. bescii* using the original unstable genetic background (Chung et al., 2014a). This enzyme reduces acetyl-CoA to ethanol (Fig. 1). The resulting recombinant strain generated 14.0 mM and 12.8 mM ethanol, respectively, from crystalline cellulose and switchgrass at 60 °C (Chung et al., 2014a). The *adhE* and *adhB* (NADPH-dependent bifunctional alcohol dehydrogenase) from *Thermoanaerobacter pseudethanolicus* 39E (T_{opt} 65 °C) were also expressed in the unstable lineage of *C. bescii* but this resulted in the production of only 2.3 mM and 1.4 mM, respectively, from crystalline cellulose at 75 °C (Chung et al., 2015). However, these titers are well below levels required for the industrial scale use of *C. bescii*, which is a minimum of 900 mM (40 g/L) (Huang and Zhang, 2011).

The AdhE enzyme requires NADH as the reductant for ethanol production and while the glycolytic pathway of *C. bescii* does generate NADH, the conversion of pyruvate to acetyl-CoA, the substrate for AdhE, produces reduced ferredoxin (Kataeva et al., 2009) (Fig. 1). One potential strategy to improve ethanol production in *C. bescii* is to enable the transfer of electrons from reduced ferredoxin to NADH. An enzyme with this capability commonly found in ethanol-generating thermophiles is the energy-conserving reduced ferredoxin NAD oxidoreductase (Rnf). This enzyme couples electron transfer from reduced ferredoxin to NAD to the generation of an ion gradient across the plasma membrane. However, *C. bescii* does not contain the six genes (*rnfCDGEAB)* that encode the Rnf complex (Biegel et al., 2011; Hemme et al., 2011; Kataeva et al., 2009; Yang et al., 2010).

In this study, we compared ethanol production by *C. bescii* heterologously-expressing *C. thermocellum adhE* in the original strain and in the more genetically-stable background strain. In addition, we attempted to further modify these strains by the heterologous expression of the six genes encoding the Rnf complex from *Thermoanaerobacter* X514 (T_{opt} 60 °C: (Roh et al., 2002)) to examine if redox balancing affected ethanol production. It should be noted that only single genes encoding cytoplasmic proteins have been heterologously-expressed previously in this organism and so successful expression of the six genes encoding the membrane-bound Rnf was a significant accomplishment. The results here revealed that the genetic background, the presence of Rnf and growth conditions all influenced carbon and electron flow to ethanol in *C. bescii* and, in combination, a more than five-fold improvement in ethanol production from crystalline cellulose was achieved compared to the previous report (Chung et al., 2014a). As such, this paves the way for more sophisticated metabolic engineering strategies with this unique microorganism and illustrates its significant potential for CBP of renewable biomass.

2. Materials and methods

2.1. Culture conditions

C. bescii was grown under anaerobic conditions in modified DSM 516 medium (C516) as described previously (Lipscomb et al., 2016), with 5 g/L growth substrate at 60 °C unless otherwise noted. For competent cell preparation, cultures were grown at 75 °C in low osmolarity defined medium with amino acids (LOD-AA) under argon, as described (Chung et al., 2012; Farkas et al., 2013). Recovery and selection were performed using the C516 medium under a headspace of 80% (v/v) nitrogen and 20% (v/v) carbon dioxide (Lipscomb et al., 2016). Uracil auxotrophic strains were grown in the presence of 20 µM uracil. Kanamycin and 5-fluoroorotic acid (5-FOA) were used at concentrations of 50 µg/mL and 4 mM, respectively (Lipscomb et al., 2016). A solid growth medium was used during strain purification that was generated from C516 medium, as described (Lipscomb et al., 2016) for growth at 70 °C over 36–48 h. Glucose, xylose, beechwood xylan, and Avicel PH-101 were obtained from Sigma. Switchgrass was sieved 20/80-mesh fraction (provided by Dr. Brian Davison, Oak Ridge National Laboratory, Oak Ridge, TN).

Fermentation cultures were grown at 500 mL scale using the DASGIP parallel bioreactor system with custom heating jackets to maintain growth temperatures between 59 and 61 °C. Modified DSM 516 medium was also used with 20 g/L cellulose (Avicel) as the growth substrate. The culture was sparged at 2 L/h with 80% (v/v) nitrogen and 20% (v/v) carbon dioxide and stirred at 150 rpm. pH was maintained at 7.0 (25 °C) through the addition of 10% sodium bicarbonate.

Table 1
Strains used in this study.

Strain Name	Genotype	Parent Strain	Reference
JWCB032	*ΔpyrFA, ldh::ISCbe4, Δcbe1, $P_{S\text{-}layer}$ Cthe-adhE*	JWCB018	(Chung et al., 2014a)
MACB1034	*ΔpyrE, Δldh*	MACB1018	(Lipscomb et al., 2016)
MACB1052*	*ΔpyrFA, ldh::ISCbe4, Δcbe1, $P_{S\text{-}layer}$ Cthe-adhE $P_{BF\text{-}H2ase}$ rnfCDGEAB*	JWCB032	This study
MACB1058	*ΔpyrE, Δldh,* $P_{S\text{-}layer}$ *Cthe-adhE*	MACB1034	This study
MACB1062	*ΔpyrE, Δldh,* $P_{S\text{-}layer}$ *Cthe-adhE $P_{BF\text{-}H2ase}$ rnfCDGEAB*	MACB1058	This study

2.2. Strain and plasmid construction

Table 1 contains a list of the strains generated in this study. Plasmids were constructed from PCR products using NEBuilder® HiFi DNA Assembly Master Mix (New England BioLabs). PCR was performed using Takara PrimeSTAR Max DNA polymerase (Takara R045A). Genomic DNA, plasmid DNA, and PCR products were purified with kits from Zymo Research and Stratagene. The templates for PCR were either previously sequenced plasmids or genomic DNA from *C. bescii*, *C. thermocellum*, or *T.* sp. X514. All primers used in this study can be found in Table S1 and plasmids constructed for this study can be found in Fig. S1. Plasmids were cloned into NEB 10-beta competent *E. coli* (New England BioLabs C3019I), followed by Sanger sequencing through GeneWiz. Plasmids for insertion into *C. bescii* strains, still expressing the *cbeI* restriction enzymes, were methylated prior to transformation, as described (Chung et al., 2012). Methylation was verified by protection from digestion with *HaeIII* restriction enzyme (New England BioLabs).

Competent *C. bescii* cells were generated, as described (Lipscomb et al., 2016). These were transformed by electroporation with Bio-Rad Gene Pulser with a voltage of 1.8–2.2 kV a resistance of 400–200 Ω and capacitance of 25 μF. Cells were transferred to 70 °C recovery medium immediately after electroporation and 5 mL samples transferred to selective medium, containing kanamycin, at intervals between 0 and 2 h of recovery and incubated at 75 °C until growth was observed, usually between 24 and 72 h. Transformants were screened for genomic integration of the plasmid and colony purified from solid medium at least once prior to counter selection for plasmid loss. Counter selection was performed on solid medium containing 5-FOA and 20 μM uracil. Final strains were confirmed by sequencing of the Athe_0949 locus (GeneWiz).

2.3. Quantitative reverse transcriptase polymerase chain reaction (qPCR)

RNA was harvested from 50 mL cultures of *C. bescii* strains grown to mid-exponential phase by phenol:chloroform extraction, followed by precipitation with isopropanol. Turbo DNA-*free* Kit (Ambion AM1907) was used to remove genomic DNA and RNA was subjected to a second round of phenol:chloroform extraction followed by isopropanol precipitation. cDNA was synthesized using the Agilent Affinity Script QPCR cDNA synthesis kit (Agilent #600559). RNA was quantified using a Thermoscientific NANODROP 2000c spectrophotometer. Quantitative reverse transcription PCR, (qPCR) was performed using the Brilliant III Ultra-Fast SYBR® Green QRT-PCR Master Mix (Agilent #600882) run on an Agilent MX3000p qPCR instrument and analysis was performed using the MxPro software (Agilent). Controls without reverse transcriptase were verified to have no amplification prior to use of cDNA for experimental quantification. Primers can be found in Table S1.

2.4. Enzymatic activity assays

Whole cell extracts were prepared from mid-exponential cultures of *C. bescii* strains grown on C516 media, with glucose as the carbon source either in 50 mL bottle cultures or in a 20 L fermentor, as described above. Cells were harvested by centrifugation at 6000*g* for 10 min or by continuous centrifugation, and immediately frozen in liquid nitrogen and stored at -80 °C. Extracts were prepared anaerobically in a Coy chamber. Whole cell extracts were prepared from 50 mL cultures by suspending cells in 100 mM phosphate buffer pH 7.0 with 5 μM ferrous sulfate and 2 mM dithionite, as described (Zheng et al., 2015). Cells were disrupted by sonication for 3 × 10 s at a maximum of 40 W with 1 min between each round of sonication. Membrane fractions generated by suspension of 5 g of cells from exponentially growing 20 L fermentors in 50 mM MOPS buffer pH 7.0 with 2 mM dithionite. Cells were lysed using 1 mg/mL lysozyme and sonication. Membrane and cytoplasmic fractions were separated anaerobically by ultra-centrifugation at 100,000*g* for 1 h, followed by two washes with an additional volume of buffer and an additional 1 h of ultra-centrifugation. Membranes were suspended in buffer by sonication before and after each wash.

Both steps of the AdhE reaction were measured with aldehyde dehydrogenase (ALDH) representing the acetyl-CoA dependent reaction and alcohol dehydrogenase (ADH) representing the acetaldehyde dependent reaction. These were measured at 60 °C in anaerobic cuvettes containing the following: 2 mL 50 mM MOPS buffer pH 7.0, 5 μM ferrous sulfate, and 0.5 mM NADH or NADPH. Reactions were started by the addition of either 0.35 mM acetyl-CoA (ALDH activity) or 10 mM acetaldehyde (ADH activity); an extinction coefficient of 6.22 mM^{-1} cm^{-1} was used for NADH at 340 nm. Rnf activity was measured in membrane fractions of wild-type, MACB1052 and MACB1062 strains. This activity was measured at 60 °C in anaerobic cuvettes containing the following: 2 mL 50 mM MOPS buffer pH 7.0, and 1 mM benzyl viologen (BV). Reactions were started by the addition of 1 mM NADH or NADPH; an extinction coefficient of 7.4 mM^{-1} cm^{-1} was used for reduced BV at 600 nm. Hydrogen uptake activity was measured for all membrane fractions to confirm similar activities in all strains. This was measured through the reduction of BV at 75 °C in anaerobic cuvettes which were flushed for 10 min with 100% hydrogen to give a hydrogen headspace. Reactions were started by the addition of membrane fractions and absorbance at 600 nm was measured. Cytoplasmic contamination was determined through pyruvate oxidoreductase activity, measured by pyruvate-dependent reduction of methyl viologen (MV), which was measured anaerobically at 75 °C in cuvettes containing: 2 mL EPPS pH 8.4, 0.2 mM CoASH, 0.4 mM thiamine pyrophosphate, 2.0 mM $MgCl_2$, 1.0 mM MV. The reaction was started by the addition of 10 mM pyruvate and an extinction coefficient of 13.0 mM^{-1} cm^{-1} was used for reduced MV at 600 nm. For all assays, anaerobic conditions were maintained by the addition of trace amounts (< 2 mM) of sodium dithionite. In all cases, activity was calculated as the difference in rate after the addition of substrate and specific activity is presented as μmol/min/mg of protein.

2.5. Fermentation analysis

Acetate, glucose, cellobiose, and pyruvate were measured in culture supernatant by high performance liquid chromatography (HPLC) on a 2690 separations module (Waters), equipped with a Bio-Rad fermentation monitoring column (Bio-Rad #125-0115), a photodiode array detector (model 996; Waters) and a refractive index detector (model 410; Waters). A mobile phase of 5 mM sulfuric acid at a flow rate of 0.5 mL per min was used and concentrations were determined by comparison to standards. Culture supernatant was acidified to a final concentration of 0.1 M sulfuric acid. Ethanol and acetoin were quantified using an Agilent 7890 A Gas-Chromatography instrument, equipped with a Carbowax/20 m column and an FID detector.

Culture supernatant was acidified prior to analysis to a final concentration of 100 mM maleic acid prior to injection. Residual Avicel from 500 mL fermentations was measured as described (Yang et al., 2009). Cell densities were monitored using a Petroff-Hauser counting chamber.

Carbon balances were determined as described (Basen et al., 2014). Briefly, carbon consumed was determined by the glucose equivalents utilized given the measured residual Avicel, carbon recovered was the sum of the measured end products, acetate, ethanol, and pyruvate, as well as glucose remaining in the medium. Carbon dioxide production was calculated based on one molecule released for every molecule of acetate or ethanol produced. Biomass was calculated based on protein estimation by the Bradford method compared to a BSA standard (Bio-Rad).

3. Results

3.1. Construction and biochemical properties of the ethanologenic strains

The first goal was to determine if the two genetic lineages of *C. bescii* that are available for metabolic engineering showed any differences in their ability to produce ethanol by the heterologous expression of *adhE*. The second goal was to determine if in either lineage ethanol production could be enhanced by the co-expression of Rnf (ferredoxin NAD oxidoreductase). Rnf generates NADH from the reduced ferredoxin produced during sugar fermentation for the NADH-dependent production of ethanol. The two available genetic lineages of *C. bescii* are the original strains derived from JWCB005 (Chung et al., 2012; Lipscomb et al., 2016) and the new strain MACB1018 (Chung et al., 2012; Lipscomb et al., 2016). The latter lineage has been shown to be much more stable than the former in terms of overall genome arrangement and insertion elements, particularly involving the active IS*Cbe4* element (Williams-Rhaesa et al., 2017).

Strains were generated in both lineages to investigate the effects of genome stability and co-expression of Rnf on ethanol production (Table 1). Strain JWCB032 has been characterized in a previous study (Chung et al., 2014a) and it heterologously expresses the *adhE* from *C. thermocellum* (Ct*adhE*), which is the major enzyme responsible for ethanol production in this organism (Lo et al., 2015). JWCB032 was also used as the parent strain for the insertion of the *rnfCDGEAB* genes encoding Rnf from *Thermoanerobacter* sp. X514 (Tx*rnf*), to give MACB1052*, where the asterisk indicates that it is derived from a JWCB strain. In the MACB1018 background, the Δ*ldh* strain, MACB1034, was selected to act as the parent strain and was modified in two steps: first the addition of the Ct*adhE* generating strain MACB1058, followed by the insertion of the Tx*rnf* genes at the same locus to give MACB1062 (Fig. S2). Note that all of the strains under study lack lactate dehydrogenase (*ldh*; Table 1) and therefore do not produce lactate as an end product.

In both genetic backgrounds, the Ct*adhE* gene was under the control of the promoter of the high level constitutively-expressed gene encoding the S-layer protein. The Tx*rnf* genes were expressed by the promoter element upstream of Athe_1295, which is responsible for the expression of the bifurcating hydrogenase (Athe_1295–1299). This enzyme is responsible for most of the hydrogen production during fermentative growth of *C. bescii* (Fig. S2) (Cha et al., 2016). Expression of the Ct*adhE* and Tx*rnfE* genes was confirmed by qPCR relative to the highly-expressed constitutive *gapdh*, which encodes the glycolytic enzyme glyceraldehyde-3-phosphate dehydrogenase. Surprisingly, the expression of the Ct*adhE* gene was dramatically different in the two background lineages, with expression in the JWCB032 lineage strains approximately 4% of the expression of *gapdh,* while in the strains in the MACB1058 lineage expression was approximately 3-fold greater than that of *gapdh* (Fig. 2**A**). It should be noted that the genome location of the Ct*adhE* in these strains is not the same (see **Discussion**) and this may play a role in the observed differences in expression, despite the fact that both genes were under control of the same promoter. In the two new strains that also encoded the Tx*rnf* operon, Tx*rnfE* expression was similar to *gapdh* expression in MACB1052*, with expression in MACB1058 approximately half of that of *gapdh* (Fig. 2**B**).

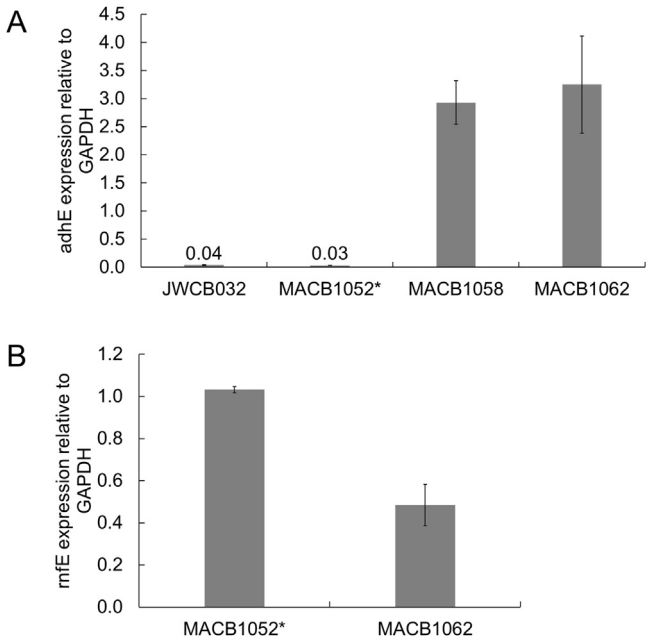

Fig. 2. Expression of the *adhE* from *C. thermocellum* (A) and the *rnfE* from *T.* sp. X514 (B) relative to the native *gapdh* in *C. bescii* ethanol production strains.

Fig. 3 shows the specific enzyme activities of bidirectional AdhE and Rnf for strains JWCB032, MACB1052*, MACB1058 and MACB1062. AdhE activities were measured in the physiologically-relevant forward direction using either acetyl-CoA or acetaldehyde reduction by NADH. These are referred to as ALDH and ADH activities, respectively. For all strains, the measured ALDH and ADH activities were comparable (Fig. 3**A**) and they were also specific to NADH as no activity was observed when NADPH replaced NADH (data not shown). In accord with the measured expression levels of Ct*adhE* in JWCB032 and MACB1052*, both had much lower specific activities in cell-free extracts (0.46–0.83 μmol/min/mg) when compared to strains from the more recent lineage, MACB1058 (3.16–3.65 μmol/min/mg) and MACB1062 (1.69–2.01 μmol/min/mg) (Fig. 3**A**).

Rnf is a membrane-bound enzyme and its activity was measured by NADH-dependent reduction of the dye benzyl viologen (BV) in washed membrane fractions rather than cell-free extracts. This eliminated contaminating BV-associated activities in the cytoplasm, e.g., from the bifurcating hydrogenase (Fig. 1). As controls, the activities of the cytoplasmic enzyme pyruvate ferredoxin oxidoreductase (POR) and of the membrane-bound hydrogenase were measured, and these confirmed that cytoplasmic contamination of the membrane fraction was below 10% (Table S2). The *C. bescii* genome does not contain homologs of the Rnf genes and accordingly membranes prepared from wild-type cells had no detectable Rnf activity (< 0.1 μmol/min/mg; Table S2). However, Rnf activity was readily detected in the membranes of both MACB1052*(7.18 μmol/min/mg) and MACB1062 (1.14 μmol/min/mg) (Fig. 3**B**). Once more, these activity results are in general agreement with transcriptional data where the expression of *rnfE* in MACB1052 * was more than twice that measured in MACB1062.

3.2. Ethanol production by the new C. bescii strains

Having confirmed that both AdhE and Rnf are active in both genetic backgrounds of *C. bescii*, the ethanol production of all four strains was

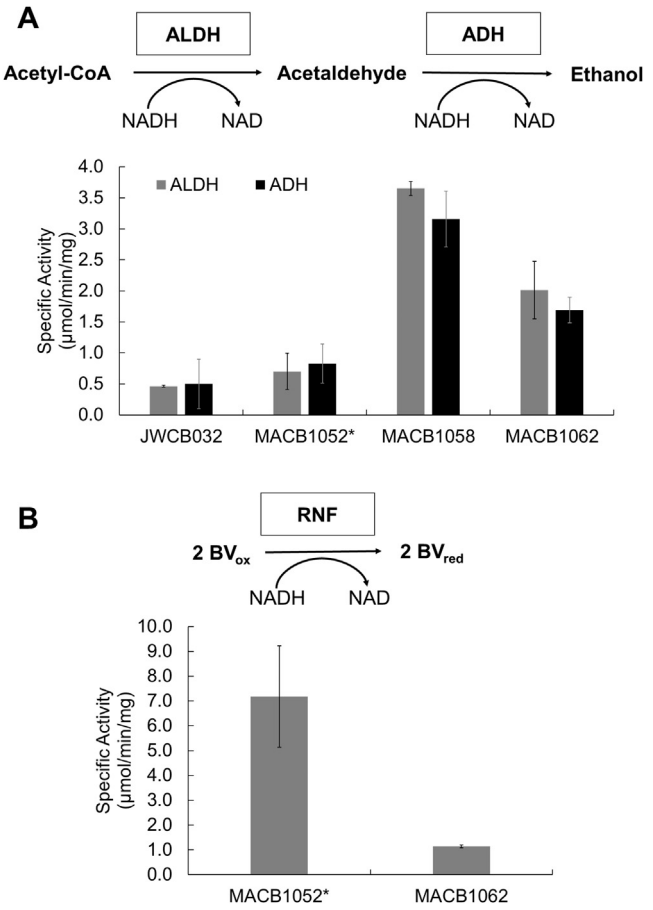

Fig. 3. Enzyme activities in cell-free extracts of *C. bescii* ethanol production strains. Assays were conducted in the direction shown. Error bars represent the standard deviation (n = 3) A) AdhE activity measured in whole cell extracts as separate reactions with Acetyl-CoA reduction shown as ALDH activity and acetaldehyde reduction shown as ADH activity. Both reactions were measured by following the oxidation of NADH to NAD. B) Rnf activity was measured in washed membranes for MACB1052* and MACB1062 by following the NADH dependent the reduction of benzyl viologen (BV).

investigated. These strains contained AdhE in the original genetic background strain with (MACB1052*) and without (JWCB032) co-expression of Rnf, and in the new genetic background with (MACB1062) and without (MACB1058) co-expression of Rnf. The strains were initially grown in closed bottles on glucose at 60 °C for 48 h (Fig. 4). As expected, under these conditions, no ethanol was detected from either parent strain, JWCB018 (old lineage) and MACB1034 (new lineage, data not shown), while ethanol was detected in all of the other strains. As shown in Fig. 4, strains in the MACB1034 background produced almost three times as much ethanol per glucose consumed as strains in the JWCB018 background. It is likely that this increase is due to the higher expression level of Ct*adhE* and the corresponding

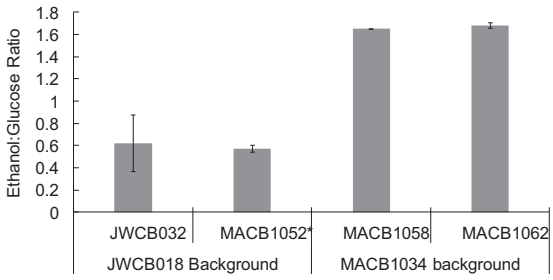

Fig. 4. Ethanol per glucose consumed at 60 °C from 50 mL scale cultures containing the *C. thermocellum adhE* in the MACB1034 background (MACB1058, MACB1062) or the JWCB018 background (JWCB032, MACB1052*).

increased AdhE activity in the MACB1034 background strains. However, under these growth conditions, co-expression of Rnf did not significantly affect ethanol production. The two strains based on the new lineage, MACB1058 (with AdhE) and MACB1062 (with AdhE and Rnf), which had superior ethanol production, were further characterized in closed cultures.

The two new MACB strains were grown between 55 and 75 °C at 5 °C increments to determine the optimal temperature for ethanol production. The highest ethanol concentration was produced between 55 and 65 °C for both strains (Fig. 5**A**). No ethanol production was observed for the parent strain, MACB1034, as expected, and none of these strains produced ethanol at 75 °C (data not shown). This suggests that AdhE is inactive at this temperature, consistent with the much lower growth temperature optima of *C. thermocellum* (60 °C) as well as a previous characterization of the Ct*adhE* expressed in *C. bescii* (original lineage: (Chung et al., 2014a)). Acetate production for strains MACB1058 and MACB1062 declined proportionally with increasing ethanol production, while slightly more acetate was produced by the parent strain MACB1034 with increasing growth temperature (Fig. 5**B**) presumably as a result of increased growth (the optimum is 78 °C).

Surprisingly, the C_4 compound acetoin was produced by all three strains at the lower temperature, being more pronounced in the ethanol production strains (~ 3 mM was produced) compared to the parent strain (~0.5 mM; Fig. 5**C**). Acetoin production was slightly lower in strain MACB1062 expressing the Tx*rnf* compared to its parent strain, MACB1058, lacking Rnf (Fig. 5**C**). Pyruvate (C3) was also detected in the growth medium of all three strains, although at lower concentrations than acetoin (Fig. S3). There was a slight increase in pyruvate produced at temperatures below 65 °C, from less than 0.5 mM at 70–75 °C to between 0.5 and 1 mM at the lower temperatures. Differences between strains were not statistically significant. As expected, due to the overall increase in the amount of products generated by the two ethanol producing strains, they consumed more glucose (20–25 mM) compared to the parent (~10 mM; Fig. 5**D**). At 75 °C, where no ethanol was produced, all strains consumed the same amount of glucose and produced approximately the same concentrations of end products (Fig. 5**A-D**).

The effect of carbon source on ethanol production by the two strains containing AdhE (± Rnf) was investigated at 60 °C using glucose, xylose, xylan, crystalline cellulose (Avicel), and unpretreated switchgrass. The two strains generated similar amounts of ethanol on all substrates (ranging from 18 to 32 mM), with the notable exception of switchgrass, where ~ 6 mM ethanol was generated, presumably because of the recalcitrance of the feedstock (Fig. S4). This was in spite of the fact that switchgrass yielded a comparable amount of acetate to that generated on glucose, yet the amount of ethanol was about 4-fold less than on glucose (Fig. S4). In contrast, growth on cellulose and xylan, the two major carbohydrate components of switchgrass, yielded about twice the amount of acetate and from 4 to 6 times the amount of ethanol. Interestingly, growth on switchgrass yielded no detectable acetoin or pyruvate in the growth media (data not shown), while on cellulose and xylan both of these end products were generated in the 0.5–2.0 mM range (Fig. S4).

3.3. Effect of fermentation conditions on ethanol production

All studies of ethanol production by *C. bescii* described to date were carried out in shaken, closed bottles with no pH control. As described above, the new ethanol-producing strains under these conditions produced more ethanol per glucose consumed (Fig. 4) compared to previous studies, presumably due to improved Ct*adhE* expression (Fig. 2**A**). Previously we showed that the use of pH-controlled, sparged bioreactors significantly improved substrate utilization and organic acid production by wild-type *C. bescii* at 78 °C, its optimum growth temperature (Basen et al., 2014). Ethanol production by the two strains was therefore evaluated under these controlled conditions. Strains

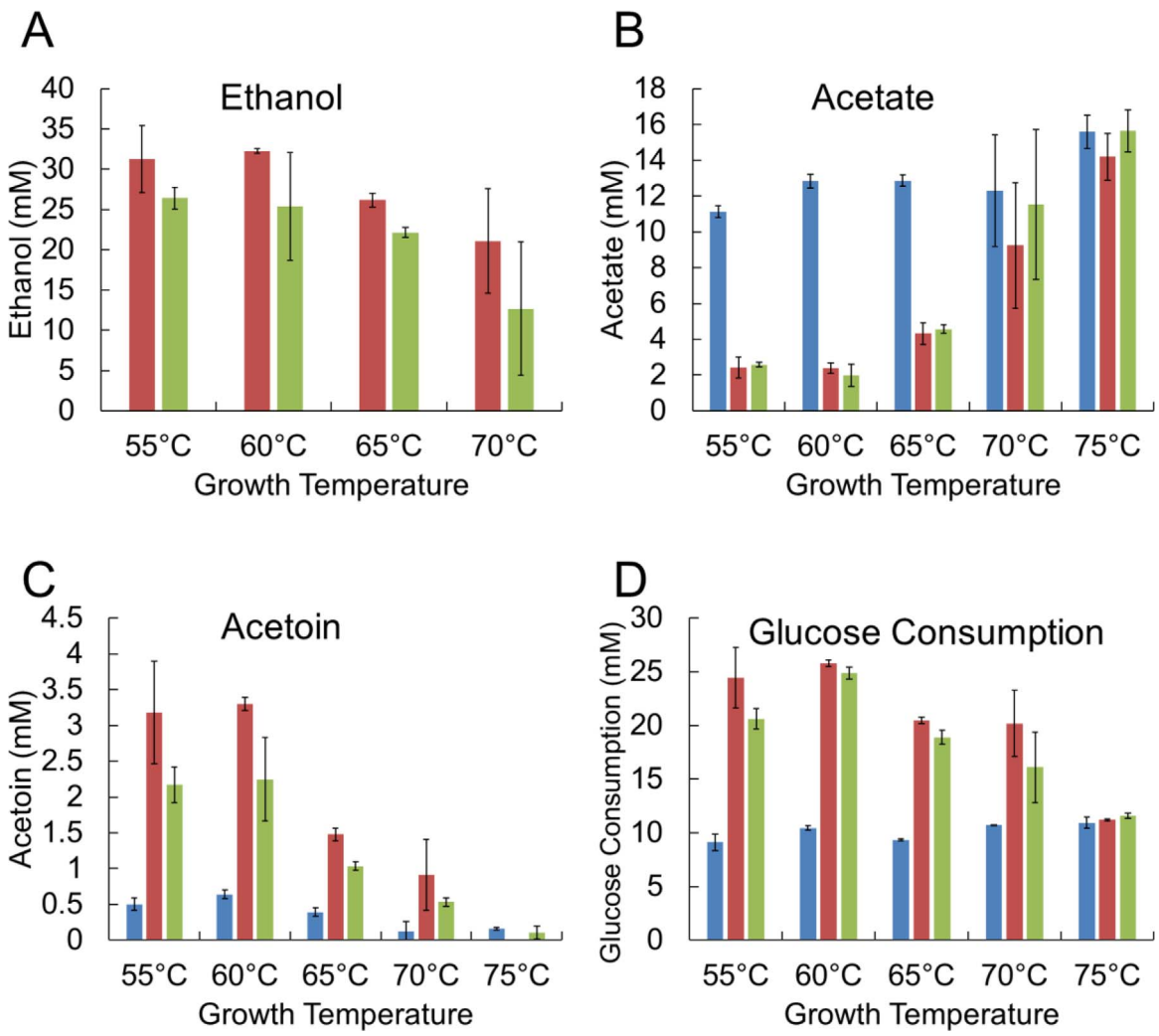

Fig. 5. Acetate (A), ethanol (B), and acetoin (C) production for 50 mL cultures with glucose, xylose, Avicel, beechwood xylan, switchgrass and poplar as the carbon sources at 60 °C for strains MACB1034 (blue), MACB1058 (red), and MACB1062 (green). Error bars represent the standard deviation (n = 3).

MACB1058 (with AdhE) and MACB1062 (with AdhE and Rnf), along with the parent strain, MACB1034, were grown on 20 g/L cellulose (Avicel) in bioreactors (0.5 L working volume) at 60 °C. With all three strains, stationary phase (~5 × 10^8 cells/mL) was reached after about 40 h and there was minimal cell lysis at least up to 200 h (Fig. S5). As anticipated, there was an increase in both ethanol and acetate production when compared to growth in closed cultures (Fig. 6). Strain MAC1058, which lacked Rnf, produced a maximum of 60 mM ethanol after 120 h, although the ethanol concentration began to decline thereafter (Fig. 6**A**). In contrast to the closed cultures, the presence of Rnf had a dramatic impact as strain MACB1062, containing Rnf, generated 75 mM ethanol, a 30% increase. Moreover, strain MACB1062 showed little if any ethanol uptake even after more than 200 h at 60 °C (Fig. 6**A**).

In contrast to the decrease in acetate production by the ethanol production strains in closed bottles, acetate production was essentially the same in the parent strain as in the two AdhE-containing strains under pH-controlled, gas-sparging conditions (Fig. 6**B**). Acetate production was lower than expected (~60 mM) when compared to that produced by wild-type *C. bescii* (127 mM acetate plus 22 mM lactate to give ~150 mM total organic acid; (Basen et al., 2014)). However, if total amount of end products for the two ethanol production strains are considered, they performed similarly to the wild-type, generating 123 mM and 139 mM in total products (ethanol plus acetate) by MACB1058 and MACB1062, respectively (Fig. 6). In addition to ethanol and acetate, significant amounts of pyruvate were also detected in the growth media of all three strains, approaching 12 mM for MACB1058 (Fig. 6**C**). Once more, Rnf made a difference since pyruvate production was significantly lower throughout the growth phase and was comparable to that seen in the parent strain. On the other hand, in contrast to what was observed in closed bottles, acetoin was not detected for any of the three strains under bioreactor growth conditions (data not shown). Glucose was also detected in the media once cells reached stationary phase and increased rapidly once ethanol production ceased in the ethanol producing strains, reaching about 8 mM in MACB1058 and about half of that in the Rnf-containing MACB1062 and in the parent strains (Fig. S5B).

Both MACB1058 and MACB1062 reached stationary phase after 40 h (Fig. S5), but continued to produce ethanol for over 150 h (Fig. 6). The rate of ethanol production was higher during growth (0.7–0.9 mM/h) and declined by more than half (0.2–0.4 mM/h) once stationary phase was reached (Table S3). However, both strains produced ethanol during growth at about twice the rate that acetate was produced by the parent strain (0.24 mM/h), even though the growth kinetics of the three strains were similar (Fig. S5). The parent strain continued to produce acetate during stationary phase at a rate also lower than that of ethanol production by the other two strains (0.16 mM/h; Table S3). With all three strains, pyruvate began to accumulate at mid-exponential phase and continued to increase during stationary phase (Fig. 6**C**). For the parent strain, pyruvate production rate

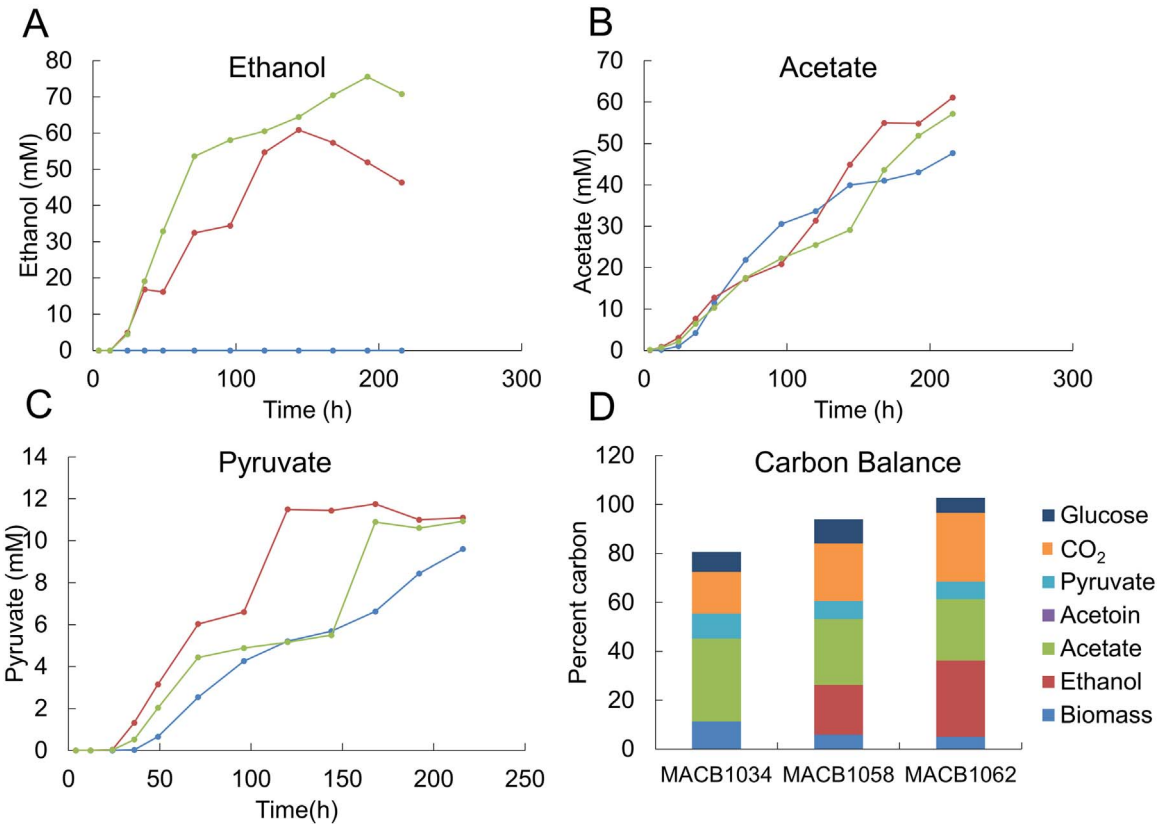

Fig. 6. Acetate (A), ethanol (B), and pyruvate(C) production and carbon balances (D) for cultures grown in 1 L bioreactors with crystalline cellulose as the carbon source at 60 °C for strains MACB1034 (blue), MACB1058 (red), and MACB1062 (green). Carbon balances were calculated based on measured glucose, pyruvate, acetoin, acetate, ethanol, cellular protein (biomass) and residual Avicel.

remained fairly constant at 0.1 mM/h (Table S3), but in both ethanol strains it ceased approximately 24 h before the maximum ethanol concentration was reached (Fig. 6**C**).

The ethanol producing strains consumed about 50% more cellulose (11.3–11.8 g/L) than the parent strain (7.6 g/L), as might be expected since they produce comparable amounts of acetate (Fig. 6**B**) but the parent does not produce ethanol (Fig. 6**A**). The carbon balance (cellulose utilized versus products detected) was closed for the Rnf strain (MACB1062, 102.8% closed) but product recovery was somewhat lower (93.9% closed) for the strain lacking Rnf (MACB1058) and much lower (80.5% closed) for the parent strain (Fig. 6**D**). The lower carbon balance for the parent strain was surprising as analysis of wild-type *C. bescii* resulted in approximately 100% closure when grown under bioreactor conditions at 75 °C, near its optimal growth temperature (Basen et al., 2014). This suggests that the parent strain generates significant amounts of an unidentified product (or products) when grown at 60 °C but not at 75 °C, a product that is not significantly generated in the ethanol strains, as these produce ethanol instead. In fact, this unknown product may be produced by AdhE-containing MACB1058 and it may account for the less than 100% carbon balance, while the presence of Rnf enables more ethanol to be produced by MACB1062 and little if any of the unknown product is generated. As shown in Fig. 1, the strains that produce ethanol generate less ATP than the parent that produces acetate. Consequently, the carbon balances reveal that in the ethanol production strains, a lower percentage of the cellulose carbon is used for cell biomass production (Fig. 6**D**).

4. Discussion

The goal of this work was to increase ethanol production in *C. bescii* by heterologous expression of the membrane-bound Rnf complex, which reduces NAD using reduced ferredoxin and should therefore yield a more redox balanced ethanol-producing pathway (Fig. 1). The presence of Rnf in the more stable genetic lineage resulted in the production of 75.5 mM ethanol under bioreactor conditions, which is 5-fold higher than the highest ethanol production previously reported from this organism (14.8 mM; (Chung et al., 2014a)). These results are very promising for the use of *C. bescii* for CBP as this ethanol titer is very similar to that reached by the cellulolytic *C. thermocellum* strain AG553, 73.4 mM, when the pathways for all other traditional fermentation products were genetically-deleted (Papanek et al., 2015). This strain was also subjected to adaptive evolution to improve the growth rate, resulting in the highest ethanol production by *C. thermocellum* to date of 580 mM ethanol (26.7 g/L; (Tian et al., 2016)). However, *C. thermocellum* has an important disadvantage compared to *C. bescii* as it is unable to utilize xylan for ethanol production (Ng et al., 1977). This is very significant because xylan represents a major fraction of the carbohydrate in plant biomass (~31% in switchgrass). In contrast, the AdhE/Rnf strain of *C. bescii* uses both xylan and xylose for ethanol production; indeed, more ethanol was produced from xylan than from cellulose (Fig. S4).

The genetic lineage of the *C. bescii* strain was important since strains in the more stable background, MACB1034, produced 1.6 ethanol per glucose consumed compared to 0.6 ethanol per glucose with the original genetic lineage JWCB018 (Fig. 4**;** (Chung et al., 2014a)). This is probably due to the lower expression of the Ct*adhE* gene, which resulted in a 2–5 fold higher specific activity of AdhE in cell-free extracts of strains MACB1058 and MACB1062 compared to JWCB032 and MACB1052*. Since the Ct*adhE* is not in the same genome location in these two sets of strains, that could be a contributing factor, especially given the proximity of this gene to a transposase (Athe_0863) and a transcriptional regulator (Athe_0864) in the JWCB018 background (Chung et al., 2014a). It is also possible that the decrease in *adhE* expression (Fig. 2**A**) could be due to the increased

insertion element activity in the JWCB018 background, which has contributed to an increase in overall genome instability (Williams-Rhaesa et al., 2017).

Although the effect of Rnf on ethanol production by *C. bescii* was not really evident in a closed culture system, it had very significant effects under bioreactor conditions with pH control and gas-sparging. Specifically, not only was there increased ethanol production by 30% when Rnf was co-expressed, there was delayed production of pyruvate and also apparently of an as yet uncharacterized compound as unwanted side-products (Figs. 4–6). These data suggest that, as we anticipated, Rnf activity results in an increased supply of NADH and this enables a higher flux of carbon from pyruvate via acetyl-CoA to ethanol (Fig. 1). Hence, ethanol production in the AdhE-containing strain appears to be NADH-limited. In the absence of Rnf, pyruvate accumulates and is either excreted or is converted to acetoin or to an unknown side product (see below). However, the Rnf-containing strain still generates acetate as a major carbon end product and its role in generating NADH may become even more important in further metabolic engineering studies, such as the deletion of either the phosphotransacetylase and acetyl-CoA synthethase or of the bifurcating hydrogenase (Fig. 1). It is not clear to what extent ATP production is increased during ethanol production by the presence of Rnf. As the Rnf used in this study is sodium dependent, this ion gradient would need to be converted by a sodium proton antiporter. *C. bescii* has an annotated antiporter encoded by Athe_1082-Athe_1086.

The production of acetoin as a side-product of fermentation at sub-optimal growth temperatures, as observed here with *C. bescii,* has also been reported with other *Caldicellulosiruptor* species, *C. sacharolyticus* (T_{opt} 70 °C: (Isern et al., 2013)), and also with the extremely thermophilic archaeon *Pyrococcus furiosus* (T_{opt} ~100 °C: (Nguyen et al., 2016)). Acetoin is generated from pyruvate by the action of acetolactate synthase and the abiotic decarboxylation of acetolactate to acetoin at high temperatures (above 60 °C). In *P. furiosus*, it was suggested that the increase in acetoin production at the lower temperature was likely due to a bottleneck in glycolysis at pyruvate due to a decrease in the rate of pyruvate oxidation by POR at lower growth temperatures (Ma et al., 1997; Nguyen et al., 2016). The results here suggest that a similar bottleneck occurs in *C. bescii* at 60 °C, resulting in pyruvate and acetoin in the growth medium, and that this can be minimized by the action of Rnf. The carbon balance analysis of the parent strain indicates that *C. bescii* also generates an as yet uncharacterized side product that presumably also stems from pyruvate, since it is minimized by ethanol production such that little if any is produced by the Rnf-containing strain (Fig. 6**B**).

Under pH-controlled growth conditions, *C. bescii* excreted pyruvate instead of acetoin (Fig. 6**C**). Lactic acid producing bacteria produce acetoin as a way of maintaining pH homeostasis in the cell, but high intracellular pyruvate concentrations are required to do this (Tsau et al., 1992). A similar effect may be occurring with *C. bescii,* where at lower growth temperatures there is a metabolic bottleneck at pyruvate and this accumulates intracellularly and is used for pH homeostasis under non-pH-controlled conditions. A possible metabolic engineering solution for the build-up of pyruvate in *C. bescii* could be the heterologous expression of pyruvate-oxidizing POR from a microorganism that has temperature optimum for growth near 60 °C. Note that increased POR activity would generate increased reduced ferredoxin, so the activity of Rnf would be even more important. Accordingly, both acetoin and pyruvate were generated in higher amounts in the strain lacking Rnf.

Herein we engineered *C. bescii* to produce ethanol but it did so optimally near 60 °C. While this is near the temperature optimum of *C thermocellum* AdhE, the ethanol producing enzyme, it is almost 20° below the optimum growth temperature of *C. bescii* (78 °C). The ethanol-producing strains at the end of fermentation had used just over half of the cellulose (~11 g/L) that was originally present in the growth medium (20 g/L). In spite of the lower growth temperature, this is very similar to that (10.6 g/L) metabolized by wild-type *C. bescii* when grown on 20 g/L cellulose (Basen et al., 2014). This contrasts with the wild-type strain at 78 °C, as this solubilized 60% of cellulose 50 g/L (Basen et al., 2014). This is not surprising, however, given the lower activity of the cellulases at 60 °C compared to 78 °C. For example, CelA, the most abundant enzyme in the secretome of *C. bescii*, retains 37% of its activity at 60 °C compared to 75 °C (Brunecky et al., 2013). Clearly, cellulose degradation is not the limiting factor in ethanol production. Similarly, *C. bescii* generated comparable amounts of ethanol from simple (glucose, xylose) and complex sugars (cellulose, xylan) although significantly less was produced from the much more recalcitrant switchgrass (in closed cultures, Fig. S4). This was expected, however, as *C. bescii* is very inefficient at biomass deconstruction at 60 °C compared to the optimal temperature of 78 °C (Yang et al., 2009).

At 78 °C, the limiting factor for growth of the wild-type strain was proposed to be accumulation of acetate (> 160 mM; (Basen et al., 2014)) and our hypothesis is that production of the less inhibitory ethanol instead of acetate would lead to increase substrate conversion. This was indeed the case at 60 °C, where the ethanol-producing strains utilized about 50% more of the initial cellulose (20 g/L) than the non-ethanol producing wild-type strain. However, to have the same effect at 78 °C, the optimum growth temperature, heterologous expression in *C. bescii* of genes encoding AdhE and Rnf that are highly active at that temperature are required. Unfortunately, potential sources of such genes are microbes that naturally produce ethanol, but none are known that do so optimally above 70 °C and only eight such bacteria are known (AdhE is not found in the archaea) that grow optimally in the 60–69 °C range (see (Keller et al., 2017)). Hence, finding more thermostable examples of AdhE and Rnf that are functional near 80 °C is key to maximizing ethanol production by *C. bescii* and particularly from recalcitrant plant biomass. Protein engineering or evolution may also be a viable strategy to improve the thermostability of these two critical enzymes.

In conclusion, ethanol production by *C. bescii* was significantly improved through the use of the new, more stable background (higher expression of Ct*adhE*), co-expression of the six genes of Tx*rnf*, and use of pH-controlled fermentor growth conditions. Interestingly, growth of *C. bescii* at 60 °C resulted in the production of acetoin and pyruvate, which was exacerbated by the expression of Ct*adhE*. Co-expression of the Tx*rnf* decreased acetoin and pyruvate production and also prevented ethanol uptake in stationary phase of controlled bioreactor cultures. Growth of *C. bescii* at these suboptimal temperatures is not ideal particularly when recalcitrant substrates are used. Thus it is critical to further optimize *C. bescii* for ethanol production at higher temperatures, including the heterologous expression of more thermostable enzymes. Additionally, future work to further alter metabolism in *C. bescii* to eliminate acetate production will be necessary.

Acknowledgements

We would like to thank Gerrit Schut, Piyum Khatibi, Jonathan Conway, Chris Straub and Laura Lee for helpful discussions. We also thank Daehwan Chung and Janet Westpheling for supplying *C. bescii* strain JWCB032. This research was supported by a grant (DE-PS02–06ER64304) from the Bioenergy Science Center (BESC), Oak Ridge National Laboratory, a U.S. Department of Energy (DOE) Bioenergy Research Center supported by the Office of Biological and Environmental Research in the DOE Office of Science and by a grant from the National Science Foundation (CBET-1264053).

Appendix A. Supplementary material

Supplementary data associated with this article can be found in the online version at doi:10.1016/j.mec.2018.e00073.

References

Basen, M., et al., 2014. Degradation of high loads of crystalline cellulose and of unpretreated plant biomass by the thermophilic bacterium *Caldicellulosiruptor bescii*. Bioresour. Technol. 152, 384–392.

Biegel, E., et al., 2011. Biochemistry, evolution and physiological function of the Rnf complex, a novel ion-motive electron transport complex in prokaryotes. Cell Mol.. Life Sci. 68, 613–634.

Brethauer, S., Studer, M.H., 2015. Biochemical conversion processes of lignocellulosic biomass to fuels and chemicals - a review. Chimia (Aarau) 69, 572–581.

Brunecky, R., et al., 2013. Revealing nature's cellulase diversity: the digestion mechanism of *Caldicellulosiruptor bescii* CelA. Science 342, 1513–1516.

Cha, M., et al., 2013. Metabolic engineering of *Caldicellulosiruptor bescii* yields increased hydrogen production from lignocellulosic biomass. Biotechnol. Biofuels 6, 1–8.

Cha, M., et al., 2016. Deletion of a gene cluster for [Ni-Fe] hydrogenase maturation in the anaerobic hyperthermophilic bacterium *Caldicellulosiruptor bescii* identifies its role in hydrogen metabolism. Appl. Microbiol Biotechnol. 100, 1823–1831.

Chung, D., et al., 2012. Methylation by a unique alpha-class N4-cytosine methyltransferase is required for DNA transformation of *Caldicellulosiruptor bescii* DSM6725. PLoS One 7, e43844.

Chung, D., et al., 2013. Construction of a stable replicating shuttle vector for *Caldicellulosiruptor* species: use for extending genetic methodologies to other members of this Genus 2013. PLoS One, 8.

Chung, D., et al., 2014a. Direct conversion of plant biomass to ethanol by engineered *Caldicellulosiruptor bescii*. Proc. Natl. Acad. Sci. USA 111, 8931–8936.

Chung, D., et al., 2014b. Deletion of a gene cluster encoding pectin degrading enzymes in *Caldicellulosiruptor bescii* reveals an important role for pectin in plant biomass recalcitrance. Biotechnol. Biofuels 7, 1–12.

Chung, D., et al., 2015. Cellulosic ethanol production via consolidated bioprocessing at 75 °C by engineered *Caldicellulosiruptor bescii*. Biotechnol. Biofuels 8, 1–13.

Conway, J.M., et al., 2016. Multi-domain, surface layer associated glycoside hydrolases contribute to plant polysaccharide degradation by *Caldicellulosiruptor* species. J. Biol. Chem. 291, 6732–6747.

Conway, J.M., et al., 2017. Functional analysis of the Glucan Degradation Locus (GDL) in *Caldicellulosiruptor bescii* reveals essential roles of component glycoside hydrolases in plant biomass deconstruction. Appl. Environ. Microbiol..

Demain, A.L., 2009. Biosolutions to the energy problem. J. Ind. Microbiol Biotechnol. 36, 319–332.

Farkas, J., et al., 2013. Improved growth media and culture techniques for genetic analysis and assessment of biomass utilization by *Caldicellulosiruptor bescii*. J. Ind. Microbiol. Biotechnol. 40, 41–49.

Hemme, C.L., et al., 2011. Correlation of genomic and physiological traits of *Thermoanaerobacter* species with biofuel yields. Appl. Environ. Microbiol. 77, 7998–8008.

Huang, W., Zhang, Y.-.H.P., 2011. Analysis of biofuels production from sugar based on three criteria: Thermodynamics, bioenergetics, and product separation.

Isern, N.G., et al., 2013. Novel monosaccharide fermentation products in *Caldicellulosiruptor saccharolyticus* identified using NMR spectroscopy. Biotechnol. Biofuels 6, 47.

Kataeva, I.A., et al., 2009. Genome sequence of the anaerobic, thermophilic, and cellulolytic bacterium "*Anaerocellum thermophilum*" DSM 6725. J. Bacteriol. 191, 3760–3761.

Keller, M.W., et al., 2017. Ethanol production by the hyperthermophilic archaeon *Pyrococcus furiosus* by expression of bacterial bifunctional alcohol dehydrogenases. Microb. Biotechnol. 10, 1535–1545.

Lipscomb, G.L., et al., 2016. A highly thermostable kanamycin resistance marker expands the tool kit for genetic manipulation of *Caldicellulosiruptor bescii*. Appl. Environ. Microbiol. 82, 4421–4428.

Lo, J., et al., 2015. The bifunctional alcohol and aldehyde dehydrogenase gene, *adhE*, is necessary for ethanol production in *Clostridium thermocellum* and *Thermoanaerobacterium saccharolyticum*. J. Bacteriol. 197, 1386–1393.

Lynd, L.R., et al., 2005. Consolidated bioprocessing of cellulosic biomass: an update. Curr. Opin. Biotechnol. 16, 577–583.

Lynd, L.R., et al., 2017. Cellulosic ethanol: status and innovation. Curr. Opin. Biotechnol. 45, 202–211.

Ma, K., et al., 1997. Pyruvate ferredoxin oxidoreductase from the hyperthermophilic archaeon, *Pyrococcus furiosus*, functions as a CoA-dependent pyruvate decarboxylase. Proc. Natl. Acad. Sci. USA 94, 9608–9613.

Ng, T.K., et al., 1977. Cellulolytic and physiological properties of *Clostridium thermocellum*. Arch. Microbiol. 114, 1–7.

Nguyen, D.M., et al., 2016. Temperature-dependent acetoin production by *Pyrococcus furiosus* is catalyzed by a biosynthetic acetolactate synthase and its deletion improves ethanol production. Metab. Eng. 34, 71–79.

Olson, D.G., et al., 2012. Recent progress in consolidated bioprocessing. Curr. Opin. Biotechnol. 23, 396–405.

Papanek, B., et al., 2015. Elimination of metabolic pathways to all traditional fermentation products increases ethanol yields in *Clostridium thermocellum*. Metab. Eng. 32, 49–54.

Roh, Y., et al., 2002. Isolation and characterization of metal-reducing *Thermoanaerobacter* strains from deep subsurface environments of the piceance basin, Colorado. Appl. Environ. Microbiol. 68, 6013–6020.

Scott, I.M., et al., 2015. A new class of tungsten-containing oxidoreductase in the genus of the plant biomass-degrading, thermophilic bacteria *Caldicellulosiruptor*. Appl. Environ. Microbiol. 81, 7339–7347.

Tian, L., et al., 2016. Simultaneous achievement of high ethanol yield and titer in *Clostridium thermocellum*. Biotechnol. Biofuels 9, 116.

Tsau, J.-L., et al., 1992. Conversion of pyruvate to acetoin helps to maintain pH homeostasis in *Lactobacillus plantarum*. Appl. Environ. Microbiol. 58, 891–894.

Williams-Rhaesa, A.M., et al., 2017. Genome stability in engineered strains of the extremely thermophilic lignocellulose-degrading bacterium *Caldicellulosiruptor bescii*. Appl. Environ. Microbiol., 83.

Yang, S.J., et al., 2009. Efficient degradation of lignocellulosic plant biomass, without pretreatment, by the thermophilic anaerobe "*Anaerocellum thermophilum*" DSM 6725. Appl. Environ. Microbiol. 75, 4762–4769.

Yang, S.J., et al., 2010. Classification of '*Anaerocellum thermophilum*' strain DSM 6725 as *Caldicellulosiruptor bescii* sp. nov. Int. J. Syst. Evol. Microbiol. 60, 2011–2015.

Zheng, T., et al., 2015. Cofactor specificity of the bifunctional alcohol and aldehyde dehydrogenase (AdhE) in wild-type and mutant *Clostridium thermocellum* and *Thermoanaerobacterium saccharolyticum*. J. Bacteriol. 197, 2610–2619.

Zurawski, J.V., et al., 2017. Bioavailability of carbohydrate content in natural and transgenic switchgrasses for the extreme thermophile *Caldicellulosiruptor bescii*. Appl. Environ. Microbiol. 83, (00969-17).